

Measurements of the Photon Total Cross Section on Protons from 18 to 185 GeV

D. O. Caldwell, J. P. Cumalat,^(a) A. M. Eisner, A. Lu,
R. J. Morrison, F. V. Murphy,^(b) and S. J. Yellin
University of California, Santa Barbara, California 93106

and

P. J. Davis, R. M. Egloff, M. E. B. Franklin,^(c) G. J. Luste,
J. F. Martin, and J. D. Prentice
University of Toronto, Toronto, Ontario M5S 1A7, Canada

and

T. Nash
Fermi National Accelerator Laboratory, Batavia, Illinois 60510
(Received 16 February 1978)

The photon total cross section on protons has been measured with high precision in the Fermilab tagged-photon beam for photon energies from 18 to 185 GeV. The cross section decreases to a broad minimum near 40 GeV, and then rises by about $4 \mu\text{b}$ over the remainder of the range. A $\rho + \omega + \phi$ vector-dominance model (normalized to low-energy data) falls below the high-energy results by 2 to $6 \mu\text{b}$, suggesting a contribution from charm-anticharm states.

Measurements below¹⁻⁴ 17 GeV of the total hadronic photoproduction cross section (σ_T) from protons have indicated a hadronlike behavior for the photon. Like most hadronic cross sections in the same energy range, σ_T decreases with energy. We have used the Fermilab tagged-photon beam⁵ to measure σ_T between 18 and 185 GeV, a domain in which most hadronic σ 's begin to rise with energy. If the photon continues to exhibit hadronlike properties, σ_T ought to reflect this rise. Moreover, charm-anticharm and perhaps higher-mass states might begin to contribute significantly.⁶

An accurate experiment with uncertainties at the level of a fraction of a percent was needed to study such effects. The basic challenge was to extract σ_T to this precision in the presence of an electromagnetic (EM) background—mostly e^+ pair production—some 180 times larger than σ_T . Our experiment was therefore *not* a transmission measurement. Hadronic events were explicitly counted, and σ_T derived from a formula like

$$\sigma_T = \frac{(\text{hadronic events})}{(\text{target protons/cm}^2)(\text{tagged photons})}. \quad (1)$$

The actual formula was more complicated, in that it included corrections for target-empty yields, beam attenuation (mainly due to pair production) in the target and windows, and the small rate of hadron electroproduction by e^+ pairs.

Primary electrons of energy E_0 radiated photons in 0.0053, 0.0107, or 0.0266 radiation lengths

(X_0) of Cu. The degraded electrons (energy E') were magnetically deflected into a scintillator hodoscope and an array of energy-measuring shower counters, thus individually tagging photons with energy $E_\gamma = E_0 - E'$ in the range $0.45E_0 < E_\gamma < 0.93E_0$. We retain for analysis only those tags consistent with a single electron; the resulting proportion of false tags (tags without a photon in the beam) was $< 0.05\%$.

The target was 1.00027 ± 0.00025 m of liquid hydrogen. Its temperature was monitored by four platinum resistors to be typically $20.4 \pm 0.2^\circ$; two independent transducer measurements of the vapor pressure yielded typical temperatures of $20.5 \pm 0.2^\circ$. An analysis found D_2 and HD contamination to be $\leq 0.05\%$. Overall, the target density times length was known to better than 0.2% .

Having dealt with the denominator of Eq. (1), we turn to the question of identifying hadronic events. The key is that in almost all EM events (pairs, γe elastic scattering, etc.) most or all of E_γ shows up in small-angle e 's or γ 's. Hadronic interactions, on the other hand, tend to produce particles at much larger angles, and rarely deposit significant electromagnetic energy near 0° . The following principles governed our experimental design: (a) polar-angle segmentation of detectors, to facilitate hadronic/EM separation; (b) coverage to $\geq 90^\circ$ in the γp c.m. frame, to catch all hadronic events—most with multiple signatures; (c) approximate scaling of detector distances with E_0 (and hence $\langle E_\gamma \rangle$) to

keep EM backgrounds in the same physical detector regions; (d) substantial overlap of E_γ ranges at adjacent E_0 settings, to provide a critical check on acceptance and detection efficiencies. Data were collected at $E_0 = 40, 60, 90, 135,$ and 200 GeV, and binned into six E_γ regions for each E_0 .

The actual detector layout⁵ is presented in Fig. 1. The central counter, C , collected all of the energy from noninteracting photons and from most pairs. π^0 -decay γ 's of successively larger angles entered hadronic detectors I (the inner ring of $G3$), $G3$, $G2$, and $S1$; other hadrons entered K (behind C), $S3$ (behind $G3$), $S2$ (behind $G2$), and $S1$. The three detector sets ($H1$, $H2$, and $H3$) were independently moved in order to provide full coverage at each E_0 . Because of the lack of space, $G2$ was removed at 40 and 60 GeV, and those two energies were run with identical configurations. For 20-GeV photons interacting at the upstream end of the target, c.m. coverage extended to only 75° ; but it exceeded 90° for almost all other cases. Data were also collected at two settings with modified geometries: 90 GeV with $H1$ and $H2$ further downstream, and 60 GeV at close to the 90-GeV configuration (with $G2$ in place).

A loose hadronic trigger was defined by a tag in coincidence with a hit in any hadronic detector. Special requirements for K discriminated against hadronic photoproduction and electroproduction occurring in C . For all such hadronic triggers, as well as for samples of all other tags, trigger information, hits in the six multiwire proportional chambers in front of $G3$, and digitized pulse heights were recorded on tape. Our off-line analysis utilized a more sophisticated event-identification procedure, and incorporated multiwire

proportional chamber (MWPC) information to assist with EM events.

The fraction of E_γ detected in C provided the major hadronic/EM separation. As can be seen in Fig. 2, EM events allowed by the loose hadronic trigger show a peak at E_C/E_γ near 1, while the great majority of hadronic events have E_C/E_γ near 0. A cut of $E_C/E_\gamma < 0.7$ has been used for most types of hadronic events. Corrections of typically $< 0.4\%$ were needed for hadronic events lost due to the cut and for EM contamination.

Many of the events with E_C/E_γ just below 0.7 were due to double bremsstrahlung. A single tagging electron may radiate two photons, either of which can interact hadronically. We have corrected for what was in effect double counting by a simple calculation to subtract the number of events in which the lower-energy photon interacted. The fractional correction was numerically nearly equal to the radiator thickness in units of X_0 , plus a term averaging 0.2% for internal (one-step) double bremsstrahlung. In addition to using $0.0107X_0$ at all energies, we collected some data at 90 GeV with $0.0053X_0$, and part at 135 and 200 GeV with $0.0266X_0$. A subtraction of the yields with $0.5 < E_C/E_\gamma < 0.7$ for the two 135-GeV runs confirmed the radiator-dependent part of the calculation to within 0.1% for the $0.0107X_0$ data.

The differences between the corrected cross sections for the various radiators and geometries are shown in Fig 3, and are consistent with zero. We have therefore averaged all data in each tagging bin. Results are listed in Table I and plotted in Fig. 4. The statistical consistency between data at similar E_γ but different E_0 (from 60 to 200 GeV) confirms at the 0.4% level the insensitivity of our results to factor-of-1.5 changes in detector positions. We estimate overall sys-

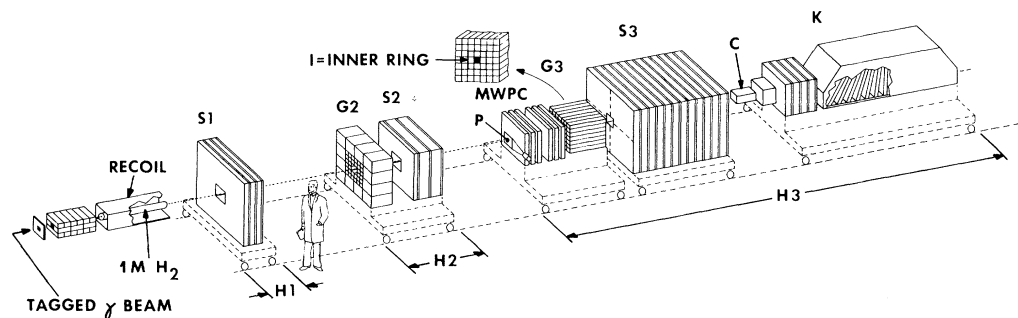


FIG. 1. Apparatus, configured for $E_0 = 90$ GeV. Vacuum extended to $H3$, with helium between the MWPC's and C , the central Pb-scintillator counter ($23X_0$). Hadronic detectors: $S1$ (three planes Pb/scintillator), $G2$ ($12X_0$ Pb glass), $S2$ (Pb/scintillator/Fe/scintillator/Fe/scintillator), $G3$ ($21X_0$ Pb glass), $S3$ and K (Fe/scintillator calorimeters).

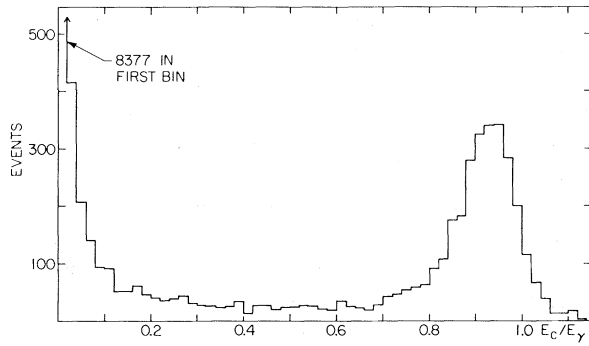


FIG. 2. Typical spectrum ($E_0 = 90$ GeV) of the fraction of E_γ detected in the central shower counter, for most events satisfying the loose hadronic trigger.

tematic uncertainties to be $\approx 0.7\%$, but E_0 -dependent uncertainties (aside from the lowest 40-GeV points) to be only $\approx 0.4\%$. A straight-line fit to the data at $E_\gamma \geq 35$ GeV yields $\sigma = (112.76 \pm 0.41) + (0.0272 \pm 0.0050)E_\gamma$, providing clear evidence of a rising cross section.

It is of interest to compare the data with the form expected from vector-meson dominance (VMD):

$$\sigma_T \propto \sum_{V=\rho, \omega, \phi} \gamma_V^{-2} \sigma_{VP} \quad (2)$$

We have computed the right-hand side of Eq. (2) from hadron-proton scattering data⁷ using the quark-model relations

$$\sigma_{\rho p} = \sigma_{\omega p} = \frac{1}{2} (\sigma_{\pi^+ p} + \sigma_{\pi^- p}), \quad (3)$$

$$\sigma_{\phi p} = \sigma_{K^+ p} + \sigma_{K^- p} - \sigma_{\pi^- p},$$

and values of γ_V^{-2} measured in A -dependent photoproduction.⁸ The result, smoothed and then

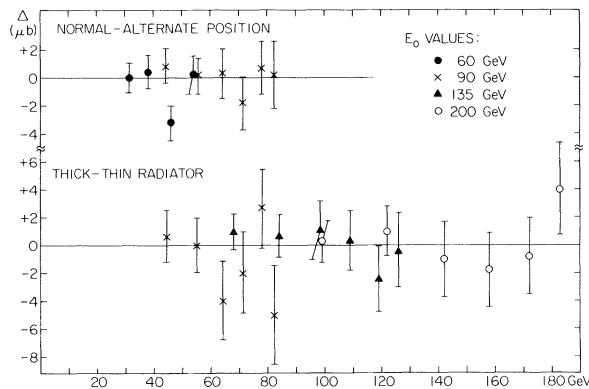


FIG. 3. Cross-section differences (Δ) vs E_γ for alternate data runs at a given E_0 . Error bars are statistical.

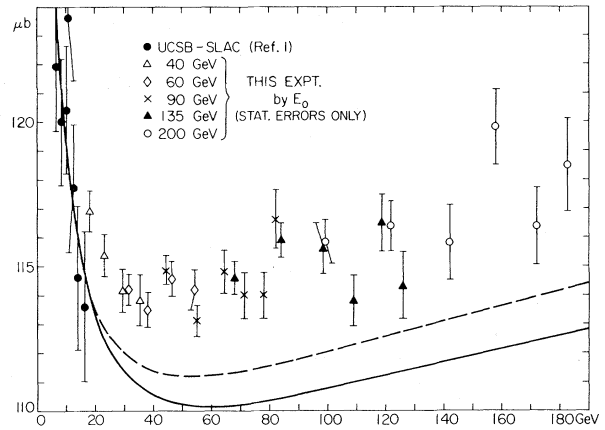


FIG. 4. σ_T vs E_γ . The curves are explained in the text.

normalized to σ_T data below 16 GeV, is plotted as the solid curve in Fig. 4. The dashed curve is obtained by the same procedure with γ_ϕ^{-2} from

TABLE I. Cross sections with statistical uncertainties.

E_0 (GeV)	E_γ (GeV)	σ (μb)	$\Delta\sigma$ (μb)
40	18.3	116.91	0.70
	23.2	115.37	0.74
	27.7	113.74	1.03
	30.9	114.34	1.09
	34.2	114.84	1.10
60	36.5	112.18	1.41
	31.4	114.19	0.55
	37.9	113.50	0.60
	43.9	114.57	0.83
	48.4	114.57	0.87
	52.6	114.25	0.88
	55.6	114.06	1.14
90	44.5	114.84	0.50
	54.9	113.11	0.54
	64.3	114.81	0.76
	71.4	114.00	0.79
	77.9	114.02	0.79
	82.4	116.61	1.02
	82.4	116.61	1.02
135	67.9	114.58	0.56
	83.9	115.89	0.61
	98.6	115.59	0.89
	109.1	113.82	0.89
	118.8	116.52	0.99
	126.0	114.30	1.13
	126.0	114.30	1.13
200	98.9	115.85	0.74
	121.8	116.37	0.87
	142.0	115.80	1.31
	157.8	119.78	1.30
	172.2	116.37	1.34
	182.7	118.49	1.62
	182.7	118.49	1.62

colliding-beam data.⁸ The curves have $\approx 1.4\%$ normalization uncertainties arising from the low-energy hadron and photon data.⁹

If the energy dependences of the $\sigma_{\nu p}$'s are representative of all components of σ_T , it is unlikely that one can obtain a curve which matches the data. Figure 4 thus suggests the presence in our data of 2 to 6 μb over what one might expect in models without charm. This excess is consistent with the charm-anticharm contribution predicted by several generalized VMD models¹⁰ and by a quantum chromodynamics calculation.¹¹

We gratefully acknowledge support from the Fermilab staff, especially the Proton and Physics Departments and the Hydrogen Target group. We also thank our technical support personnel, including M. Armstrong, D. Briggs, Y. Chan, A. Kiang, H. Nickel, D. Simmen, and R. Stuber, and students J. Gallet and C. Lauer. Valuable assistance was provided by M. G. Donnelly, and also by A. Belousov and B. Govorkov of the Lebedev Physical Institute. This research was supported in part by the U. S. Department of Energy and by the National Research Council of Canada through the Institute of Particle Physics of Canada.

^(a) Present address: Fermi National Accelerator Laboratory, Batavia, Ill. 60510.

^(b) Present address: Varian Associates, Palo Alto, Calif. 94303.

^(c) Present address: Stanford University, Stanford, Calif. 04303.

¹D. O. Caldwell *et al.*, Phys. Rev. Lett. **23**, 1256

(1969), and Phys. Rev. D **7**, 1362 (1973).

²H. Meyer *et al.*, Phys. Lett. **33B**, 189 (1970).

³T. A. Armstrong *et al.*, Phys. Rev. D **5**, 1640 (1972).

⁴S. Michalowski *et al.*, Phys. Rev. Lett. **39**, 733 (1977).

⁵Full descriptions of the tagged-photon beam and of our detectors and their calibration will be published elsewhere, and are also available in J. P. Cumalat, thesis, University of California at Santa Barbara, 1977 (unpublished).

⁶F. Hayot and H. T. Nieh, Phys. Rev. D **12**, 2907 (1975); B. L. Young and K. E. Lassila, Phys. Rev. D **12**, 3424 (1975); D. Sivers *et al.*, Phys. Rev. D **13**, 1234 (1976).

⁷A. S. Carroll *et al.*, Phys. Lett. **61B**, 303 (1976); S. P. Denison *et al.*, Phys. Lett. **36B**, 415 (1971), and Nucl. Phys. **B65**, 1 (1973); K. J. Foley *et al.*, Phys. Rev. Lett. **19**, 330 (1967); H. W. Galbraith *et al.*, Phys. Rev. **138**, B913 (1965).

⁸A. Silverman, in *Proceedings of the International Symposium on Lepton and Photon Interactions at High Energy, Stanford, California, 1975*, edited by W. T. Kirk (Stanford Linear Accelerator Center, Stanford, Calif., 1975), p. 360.

⁹The best normalization of the solid curve of Fig. 4 to all of the data plotted has a χ^2 of >74 for 33 degrees of freedom (confidence level $<10^{-4}$), even if one arbitrarily allows separate normalization constants for the present data and the data of Ref. 1. (The less reasonable dashed curve would lead to a confidence level of 2% under the same conditions.)

¹⁰F. E. Close *et al.*, Nucl. Phys. **B117**, 134 (1976); B. Margolis, Fermilab Report No. Pub-77/71-THY (unpublished).

¹¹F. Halzen and D. M. Scott, University of Wisconsin Report No. COO-881-8, 1977 (unpublished). Other quantum chromodynamic calculations yield a smaller result; see, for example, M. A. Shifman *et al.*, Phys. Lett. **65B**, 255 (1976).